Spring 2016

Quantifying the locomotion of C. elegans and their response to photo stimulation

Ian Seddon
Rollins College, iseddon@rollins.edu

Quantifying the locomotion of *C. elegans* and their response to photo stimulation.

Ian Seddon
May 2016

Faculty Sponsor: Anne Murdaugh

Rollins College
Dr. Pieczynski's Lab

Rollins College
Winter Park, Florida

Table of Contents

Abstract

Identifying the function of different locomotive genes in model organisms is crucial for genetics research. One popular approach is to analyze the behavior and motion of animals in hope of understanding subtle genetic or neural mechanisms. The nematode *C. elegans* has emerged as an increasingly popular organism for the study of sensory systems, specifically photo transduction, due to the fact it is still photosensitive without having eyes. Light stimulus has been shown to elicit evasive locomotive behavior in *C. elegans*, however little has been done to quantify this movement. Modeling the worm motion as a static sine wave, we used the parameters of wavelength, amplitude, and worm speed to differentiating between stimulated and non-stimulated worm behavior. *C. elegans* have four main modes of locomotion: straight, shallow turn, omega turn, and reversal. These three parameters were determined across all four locomotive modes for two worms. We found that worm speed is a promising parameter for differentiating between locomotive modes, and between unstimulated and photo-evasive locomotion. Due to high error, the amplitude and wavelength were inconclusive locomotive parameters.

Introduction

The human body is made up of several trillion cells, each containing deoxyribonucleic acid (DNA). DNA consists of segments of genes that determine an individual's traits, playing a role in both the physical appearance of an individual and their overall health by determining how the body functions. While most genes benefit the body, certain genes are associated with increased susceptibility to a variety of harmful health conditions. As a result, genetic research is an important field for detecting, preventing, and treating diseases associated with certain genes or genetic abnormalities.

Detecting the subtle functions of certain genes can be challenging. Typically one has to work backwards from the phenotype—the appearance or behavior of the individual—to then determine the organism's genotype, the form of the gene responsible for that characteristic (1). A common approach is to study animal behavior and correlate behavioral differences with biological mechanisms. Behavior represents how organisms interact with, and adapt to, their environment. Combining the study of animal behavior with neuroscience allows neurobiologists to hypothesize about neural structure and function. Additionally, careful behavioral analysis can help establish natural variation between organisms and narrow the scope of their studies to specific responses or populations (2).

Animals have specialized sensory systems that react to environmental stimuli such as chemicals, mechanical forces, and light. While the morphology of these sensory systems varies among different organisms, the cellular mechanisms that regulate sensory perception and processing are similar (3). For example, light is commonly detected

through photoreceptor cells in the retina. These calls form images, establish circadian rhythm, and mediate phototaxis response. Phototaxis, which refers to any directional movement in response to light, is often critical for the survival of many organisms. The most obvious behavioral output for animals is through locomotion, and so detailed analysis of their fundamental locomotory modes is a helpful tool when investigating animal response to external stimuli. The nematode *C. elegans* has emerged as an increasingly popular organism for the study of sensory systems, specifically photo transduction, due to the fact it is still photosensitive without having eyes. Light stimulus has been shown to elicit evasive locomotive behavior in C. elegans, with prolonged light exposure being lethal (4). This phototaxis response is believed to be a survival mechanism meant to keep *C. elegans* in their dark, soil environment (5). Studies have shown that phototaxis varies depending on the type and duration of light stimulant, however very little has been done to examine the parameters of motion during this movement. This study applied a simplified version of the wave model to worm locomotion and produced parameters of worm motion with and without light stimulation.

C. elegans as Model Organism

Scientists currently lack a comprehensive understanding of complex biological mechanisms, where many molecular networks operate concurrently inside our bodies (6). For example, slight genetic or neural variations in an organism are simply changes in its DNA and protein structure, which at the tissue level will change the histology, which then could lead to a behavioral change (7). To simplify this issue, geneticists are mapping the biological networks of simpler organisms such as bacteria, yeast, and worms to create

working models of how cells, organs and tissues function in humans (6). Studying these model organisms can be particularly useful when identifying, diagnosing, and treating diseases because it can take dozens of years for a genetic disorder to manifest itself in a human.

Over the past few decades, important advancements in large-scale DNA sequencing have dramatically changed the scope of genetic research. Complete genome sequences of viruses, bacteria, and yeast have been obtained along with the gene structure, gene regulation, and gene product functions of these model organisms (8). The first completed genome of a multicellular organism was obtained with the completion of the *Caenorhabditis elegans* (*C. elegans*) genome in 1998 (9). Knowing the complete genome of *C. elegans* has made the *C. elegans* nematode an ideal model organism because it has allowed scientists to easily identify and test the functionality of certain genes (11). Furthermore, as the only organism with its entire nervous system mapped out at the cellular level, scientists use *C. elegans* to explore the genetics of neural diversity (9,10). With the completion of its genome, steps have been taken to determine the function of each gene and understand how neural activity and physiology are related (11).

C. elegans research is also applicable to the study of human biology, due to the fact that the majority of human disease genes and disease pathways have been confirmed in *C. elegans* (9). Depending on the particular bioinformatics approach used, *C. elegans* gene homologues are directly comparable to 60–80% of human genes (10,14,16). In addition to its genetic similarity, the *C. elegans* worm has many practical features that make it a powerful tool for biomedical research. Although the adult hermaphrodite has only 959 somatic cells, which is miniscule compared to the trillions of human cells, it is

still biologically complex with many different organs and tissues including muscle, hypodermis, intestine, reproductive system, glands, and a nervous system containing 302 neurons (15). *C. elegans* are easy to culture: although the animals normally grow in the soil and feed on various bacteria, they can readily be raised in the laboratory on a diet of *Escherichia coli*. They reproduce quickly and abundantly, developing from eggs to adult worms in 3 days. Due to their small size, assays can be carried out in microtitre plates either on agar or in liquid. The worm is transparent and thus, with the use of *in vivo* fluorescence markers, biological processes such as axon growth, embryogenesis and fat metabolism can be visually studied in the living animal using an optical microscope. Furthermore, this organism can adapt its motion to different environments, adjust its behavior to mechanical, chemical, and thermal stimuli, and learn. (15).

C. elegans Locomotion

Due to their biological applications and ease of use, the free-living nematode *C. elegans* provides an excellent setting in which to investigate behavioral locomotory responses to external stimuli and to understand these in genetic and neural terms. On agar surfaces, *C. elegans* lie on their side, and move forward by alternatively contracting their dorsal and ventral muscles, propagating themselves in the form of a wave. These waves decay from head to tail, which contrasts sharply with that observed for typical undulatory swimmers, where amplitudes of body displacement grow from head to tail (26). The wave travels posteriorly along the body length if the worm moves forward, and anteriorly if the worm moves backward. As a result, the worm crawls and its body follows an approximately sinusoidal trajectory.

Forward movement is occasionally interrupted by stereotypical behavioral sequences, the three most common being shallow turns, reversals, and omega bends. These reorientation modes result in sharp changes in the direction of motion of the worm, two of which are shown in Figure 1. Both the shape and the speed of the worm

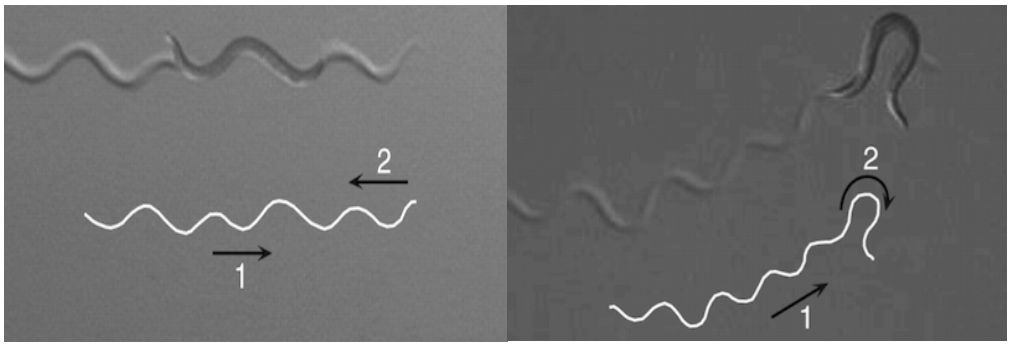

Figure 1. The typical track patterns of a reversal (left), and an omega turn (right) for crawling *C. elegens*, modified from Kim et al. (17). The sequences of motion are designated by the numbers and the arrows.

undulations change in response to the environment of the worm. For example, between sharp turns the paths of *C. elegans* consist of progressively curving segments, whose curvature is regulated by chemical and thermal stimuli (23). Additionally, these stimuli affect their locomotion by modulating the frequency of sharp turns (23). Thus, current locomotion research has focused primarily on gait analysis, and how the worms respond to their surrounding environment (17-20).

C. elegans have an adaptable motor circuit, enabling them to adjust their movement to surroundings that impose a wide range of mechanical resistance by swimming, burrowing, or crawling (18). Mechanical resistance refers to the external forces that *C. elegans* experience as they move within different mediums (18). This is particularly evident when analyzing their locomotion swimming in water versus crawling on agar surfaces. For example, the wavelength of a swimming worm is roughly twice the body length (21). When crawling on a wet surface, they endure resistive forces 10,000-fold

larger than when swimming due to an increase in surface tension and friction. Under such a dramatic increase in external load, they adapt their gait by reducing both undulation frequency (from 2 Hz to 0.2 Hz) and wavelength (from 2 to 1/2 of the overall length) (18).

Current locomotive research for *C. elegans* has varied significantly, performing either highly detailed and specific analyses or more descriptive and general studies. (13,17). For example, Schulman et al. examined the forces exerted by a *C. elegans* worm when propelling itself in different environments. The crawling force of the worm was measured using elastic pillars while the viscous forces of the environment were measured through particle image velocimetry (19). The result was a high-resolution time sequence of the drag forces felt by *C. elegans* while swimming in a buffer. After incorporating these force measurements with the resistive force theory (RFT), a simple model was established to describe the general locomotion of slender microswimmers. The drag coefficients for *C. elegans* in different mediums were calculated allowing direct calculations of the forces generated by the free swimmers (19).

However, crawling locomotion is particularly complicated when analyzing external forces because one has to account for factors such as the surface tension that holds the worm to the agar surface, the forces that incise the groove, and the variable friction and tension along and around the worm's cylindrical body (25). To overcome these obstacles, most locomotive studies have shifted the focus from force analysis to the kinematic parameters by which the worm travels.

A recent locomotive model for *C. elegans* is the piecewise harmonic curvature model, which has three fundamental assumptions (23). First, the worm controls its body

posture by propagating the curvature backwards along its body. Second, the wave is generated in the head of the worm, and varies in time. Third, the variation of the head can be described in terms of a harmonic function. Based on these assumptions, kinematic analyses have been performed to both worm trails as well as worm shape.

Stephens et al. took this idea further to show that the complex shapes that *C. elegans* assume during crawling can be represented in orientational coordinates intrinsic to the worm body (13). In this model, worm shapes were expressed as eigenmodes of a correlation matrix for orientation of body segments. Eigenmodes can be used as concise descriptors of individual movement patterns by determining the natural shapes and frequencies of an object during free vibration (28). The "eigenworm" description was one attempt at developing realistic models of worm locomotive behavior. The dynamics along these eigenworms offered both a quantitative characterization of classical worm movement such as forward crawling, reversals, and omega-turns, and evidence of more subtle behaviors such as pause states at particular postures (13). However the "eigenworms" are not intuitive, and ignored the parameter difference between different reorientation modes.

Other studies have been more general in their descriptions of locomotion, analyzing nematode behavior to determine the probability of turns, the fraction of worms that approach a chemical signal within a prescribed time, and common body postures of *C. elegans* (e.g., sinusoidal undulations and shallow, sharp, and loop turns) (35). These descriptive studies of worm motion failed to address advanced questions such as how the nervous, sensory, and motor systems of *C. elegans* work together to generate efficient propulsion and move the worm towards a food source or away from danger (23).

Padmanabhan et al. analyzed entire trails of crawling nematodes (rather than their individual body shapes) to capture sudden changes in the gait of the worm as it navigated its environment (23). The descriptions were formulated in terms of intrinsic geometric quantities (arc length and local curvature), rather than real-space coordinates, which made them much more detailed than simple shallow turns and low-amplitude undulations. From this model, all worm postures and trajectories were represented with using harmonic equations. However, as the worm reorients itself, the parameters of its sinusoidal undulations change for each locomotive mode. Thus, while this method had its merits, it was concluded that a single set of parameters cannot represent the entire path of the worm, only individual segments of the trail (23).

By analyzing animal behavior, scientists can begin to understand the structure and function of complex neural and genetic pathways. *C. elegans* worms are ideal model organisms to study stimuli response because of their ability to adapt to their surroundings. Scientists have primarily used complex locomotive models to quantify the motion of *C. elegans*, however there has been very little research on their locomotion during phototaxis (8). Current locomotive models are either general and descriptive or very specific and comprehensive, presenting their conclusions in a form that can be inaccessible to the biological community. The goal of this thesis is to investigate the phototaxis response of *C. elegans* using easily accessible locomotive parameters that help resolve this multi-audience problem.

Wave Model

General observations of *C. elegans* have revealed that their physical movements resemble that of a simple harmonic oscillator (e.g. a transverse wave). Thus, we have attempted to quantify their locomotion using wave parameters such as wavelength, velocity, amplitude, frequency, and wave number.

At a very basic level, a wave is a repeated disturbance that propagates in a medium, transferring energy from one place to another (29). In nature, these occur in common phenomena such as the sound, light, and water ripples. Figure 2 shows a 2-dimensional form of this disturbance in terms of time and amplitude.

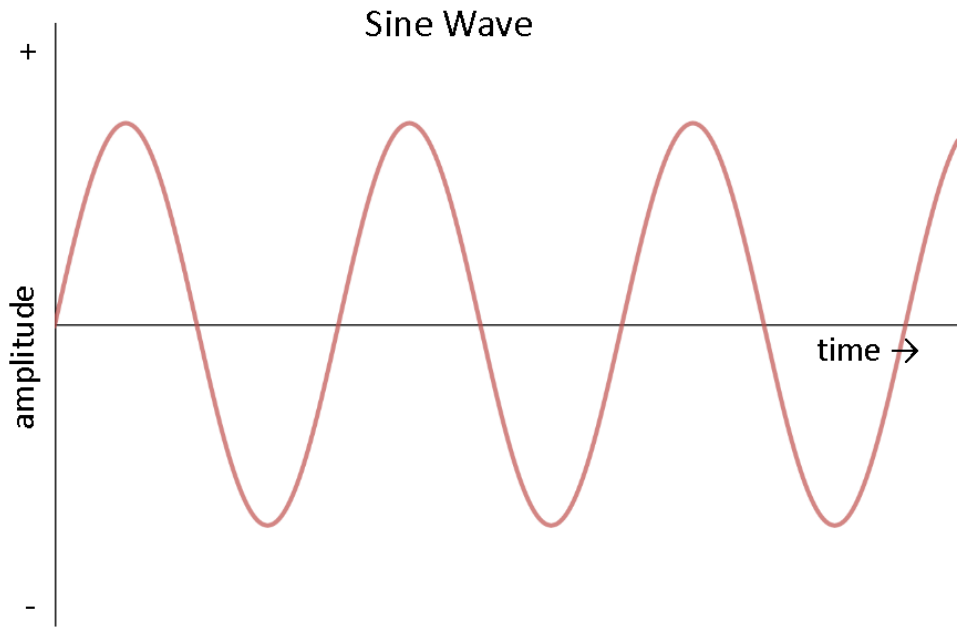

Figure 2. The spatial representation of a wave traveling in time, modified from sparkfun.com (30).

Here, the amplitude of the wave is defined as the distance A that the wave moves on either side of the equilibrium position. If the oscillations of a source are periodic and regular, then the distance between two successive amplitudes in the medium in the same

phase is defined as the wavelength. The wavelength is the distance the wave travels before repeating itself, typically referred to as one oscillation.

The time it takes for a wave to make one oscillation is known as the period (T). In some cases it is more convenient to describe the frequency of the oscillations, which is the reciprocal of the period

(1) $$f = \frac{1}{T}.$$

Frequency (f) is measured in cycles per second, but it is more useful to write frequency in terms of angular frequency (ω), which is expressed as

(2) $$\omega = 2\pi f.$$

In the absence of friction, the amplitude would remain constant. However, in a system with dissipative forces, the amplitude can vary over time.

Each time the source makes one complete cycle; a new wave is produced and continues to travel with a wave speed of v. This v depends on the properties of the medium.

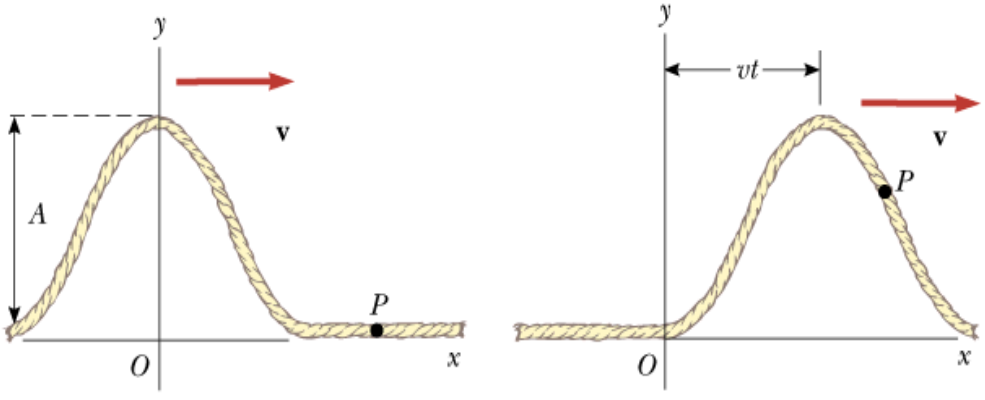

Figure 3. Diagram of a traveling wave, modified from BYU.edu (31). A) The peak of a wave at time t = 0. B) The peak of a wave shifted a distance vt after a certain amount of time.

If the period of oscillation is T, and the wave is moving at a constant speed of v, then the particle will travel a specific distance in a certain length of time. This relationship between the wave speed and the frequency, can be expressed in terms of wavelength (λ) using the equation

(3) $$\mathrm{v} = f\lambda.$$

This equation holds for any continuous wave traveling in a uniform medium. If a wave is oscillating with simple harmonic motion, then the waves will resemble a sine or cosine function. Thus, the following equation can be used to describe a traveling wave:

(4) $$y = A\sin(\mathrm{k}x - \omega t).$$

In this expression, A represents the amplitude of the wave and k represents the wave number, which can be written as

(5) $$\mathrm{k} = \frac{2\pi}{\lambda}.$$

Waves are different from oscillations in the sense that waves propagate through a medium over time. If we look at a snapshot of a sine wave in motion, it can be described in the following way:

(6) $$y = A\sin(kx).$$

When modeling the motion of *C. elegans*, we can ignore the time dependent aspect of the wave. While the body of the worm traces out the shape of a wave, the wave shape itself never moves in time. Thus, the motion of the worm does not resemble a traveling wave but a static wave as shown in Figure 4.

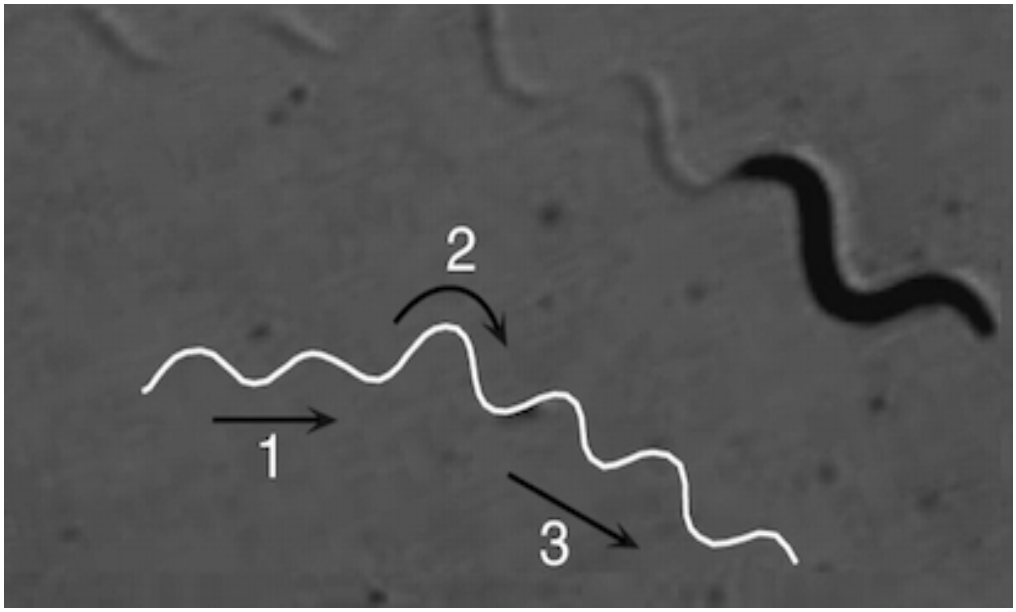

Figure 4. Diagram of a *C. elegans* performing a slight turn while propagating through a medium, modified from Kim et al. (17). The path of the worm is traced out, showing that although the worm is moving in time, the wave path it is tracing out is not.

When analyzing the movement of the worm, we track the movement of the head over time and describe the speed of the worm rather than the speed of the wave.

The minute details of *C. elegans* locomotion have not yet been quantified in a way that is accessible to the general scientific community. The end goal of this study was to produce indices of locomotive behavior for normal movement that are easily applicable for basic worm phenotypic analysis. Using videos of *C. elegans* motion, the locomotion of two worms was analyzed to determine the wavelength, amplitude, and speed of their motion. To test whether these parameters can effectively differentiate between locomotive behaviors, the parameters for four main locomotive modes were compared. Similarly, these parameters were used to analyze the difference between unstimulated movement and evasive phototaxis.

Methods

Animal Husbandry.

Wild type N2 animals used in this study were purchased from the *Caenorhabditis* Genomics Center (CGC, University of Minnesota-Twin Cities), which is funded by the NIH Office of Research Infrastructure Programs (P40 OD010440). The strains used in this study were maintained on normal growth medium (NGM) agar plates supplemented with *E. coli* strain OP-50 as previously described by Brenner (32).

Data acquisition.

Age matched N2 animals were transferred to unseeded NGM agar plates with halocarbon oil and allowed to acclimatize for five minutes. After acclimating, videos were captured using a MoticamX camera, with a resolution of 1280x1024 pixels, mounted on a Motic SMZ-171-TLED 7.5X-50X LED Trinocular Zoom Stereo Microscope (Motic Americas, BC, Canada). Images were captured using Motic Images Plus 2.0 software. To minimize the noise due to biological variability between worms, the worms were observed one at a time. The first set of videos taken was the control set (CS), which focused on one worm as it navigated the dish without any external stimuli. The second set of videos taken was the stimulated set (SS), which was used to observe any locomotive changes during phototaxis. The movement of the worm was recorded before and after the light intensity of the environment was altered. The light intensity was adjusted by momentarily obstructing the light of the microscope with a hand.

Worm Motion Analysis

Current literature has shown that the muscular wave of the worm decays from head to tail (21). Thus, to isolate fully analyze the muscular wave the motion of the worm was tracked from the head. The worm videos were analyzed using Tracker Video Analysis and Modeling Tool (Open Source Physics) by defining the head of the worm as a point mass and manually tracking its position for each frame. The position of the worm head was described using x-position and y-position coordinates by overlaying a two-dimensional Cartesian coordinate system on top of the video as shown in Figure 5.

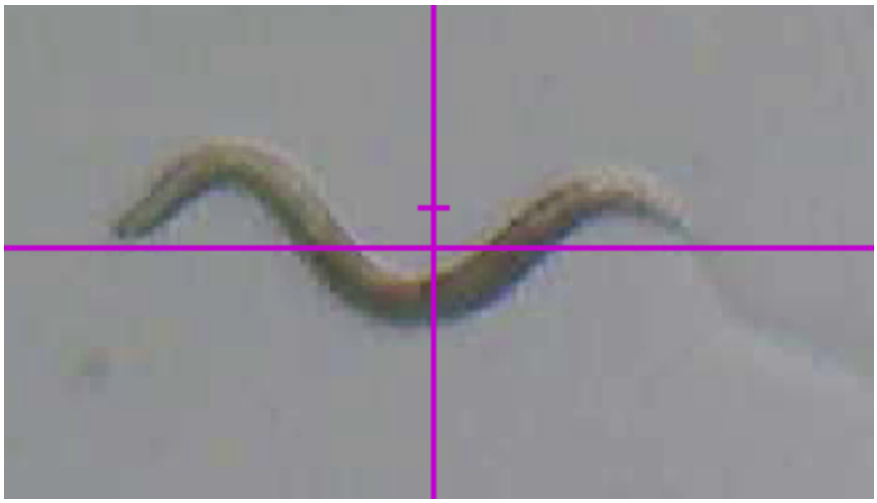

Figure 5. Schematic of the *C. elegans* with a Cartesian coordinate system overlaid on top of the image. The vertical axis is the x-axis, while the horizontal axis is the y-axis.

The coordinate system was calibrated to a scale embedded in the video, and positioned so that the worm traced out its path along the y-axis. An example of a typical worm path is shown in Figure 6.

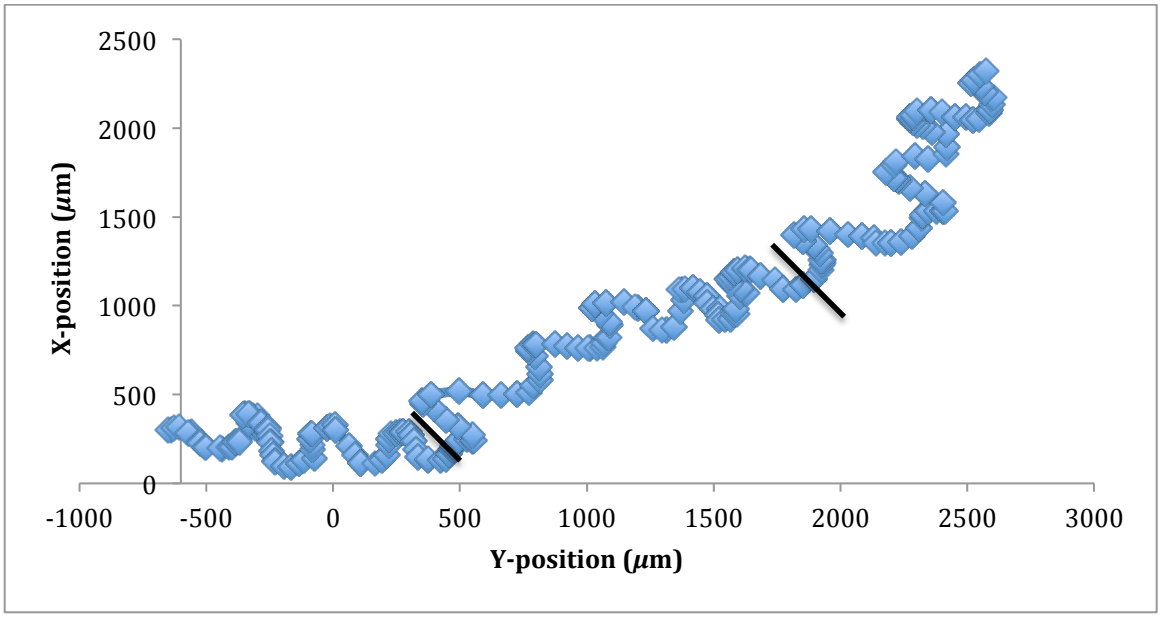

Figure 6. A typical track pattern traced out by the worm head. The worm made a shallow turn after traveling 500 μm along the y-axis and after traveling 2000 μm along the y-axis.

C. elegans move in straight lines, with three main modes of reorientation: shallow turns, omega turns, and reversals. After each reorientation, the axes of the coordinate system had to be repositioned so that the worm motion remained aligned with the y-axis. During omega turns, *C. elegans* lose their sinusoidal wave shape as they contort their bodies. Since our model only applies to sinusoidal wave motion, the data for omega turns were only taken after the head of the worm completed the omega turn. The motion of the head was then analyzed until the rest of the body completed the turn. Any subsequent motion was different locomotive mode. Any worm motion that failed to remain along the y-axis for at least two peaks was not analyzed. Any worm motion that was executed over numerous oscillations without reorientation only corresponded to one set of parameters. The final output from this Tracker software included the coordinates of the worm head for each frame, and the amount of time that elapsed between frames.

Data Analysis

From this data, graphical plots were used to determine the wavelength, amplitude, and worm speed of the worm motion for each specific locomotive mode exhibited in the videos. To find the wave speed, the y coordinates were graphed versus time. This data resembled a linear line, as shown in Figure 7.

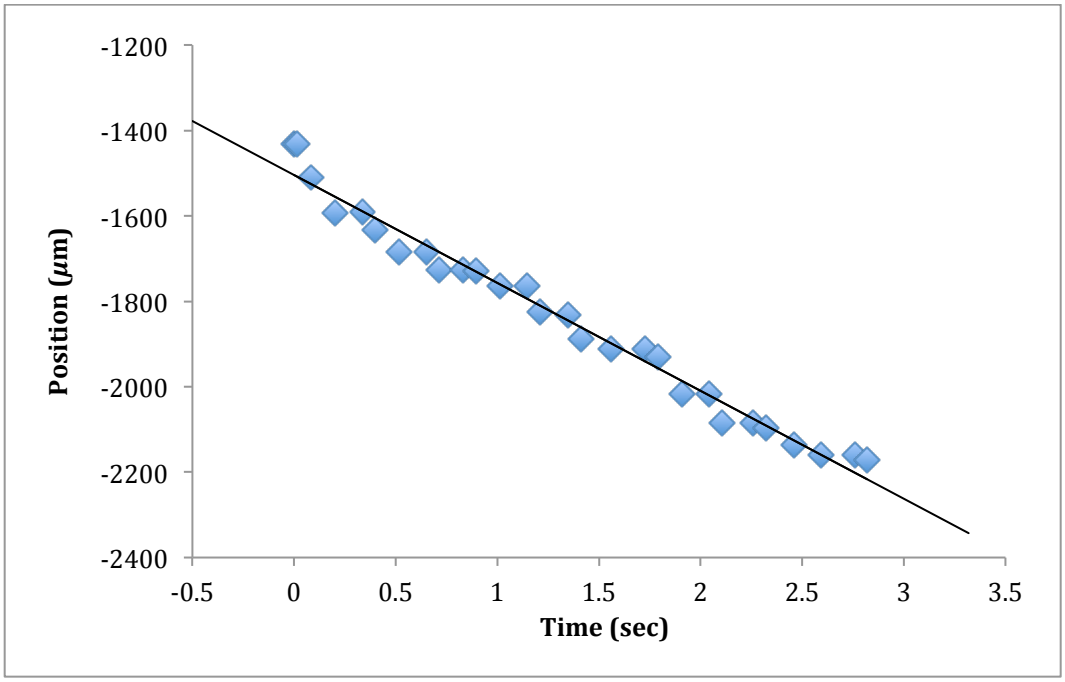

Figure 7. The motion of the worm along the y-axis over time. The linearity of the data shows that the worm is moving at a constant speed. A linear regression was used to find the slope of the line, which represents the speed of the worm.

The slope of the line represents how quickly the worm head is moving in the y-direction, which we refer to as "worm speed". A linear regression was used to find the slope of the line and the standard error of the regression was determined. To isolate the linear motion in between turns, non-linear data at the beginning and end of each plot was discarded and used for plots with different coordinate axis orientations. Thus, each plot only represents the data taken when the worm was moving in only the y-direction.

To determine the wavelength, the y-coordinates were graphed versus the x-coordinates to represent the path of the worm. An example of the worm path, independent of time, is shown in Figure 8.

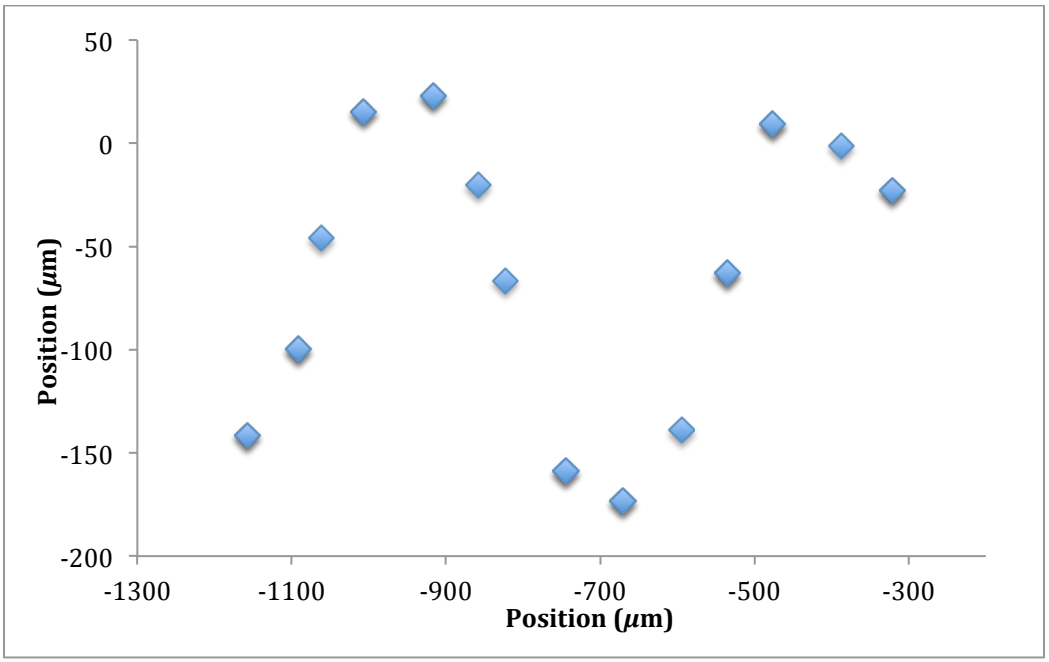

Figure 8. A graph of the worm path traced by the head. Each data point represents the position of the head for one time frame.

Due to the incremental process of data collection per frame, obtaining a smooth wave was not possible. This made it difficult to determine the exact peak of the wave, which is crucial for measuring the amplitude of the wave and the distance between peaks to determine the wavelength. To identify the peak of each curve, a Gaussian function was fit to each curve as shown in Figure 9.

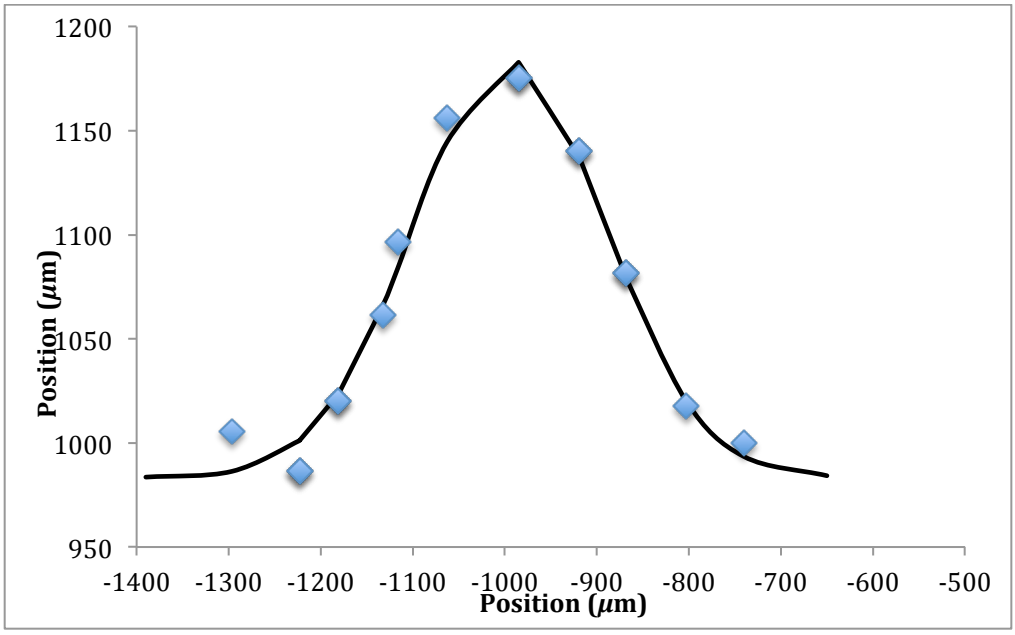

Figure 9. A graph of the worm position and the corresponding Gaussian fit. The experimental data is represented by the blue points, while the black line represents the theoretical Gaussian curve. From this line, a Gaussian equation was used to find the peak of the curve. From this peak, the wavelength and the amplitude of motion were determined.

To produce the best fit, root mean squared error analysis was performed to find the optimized constants for the following Gaussian equation:

(6) $$f(x) = B + Ae^{\frac{-(x-\mu)^2}{2\sigma^2}}.$$

Here, the B represents the baseline y-value, A represents the amplitude, μ represents the location of the peak, and σ represents the standard deviation of the Gaussian function. Using the Gaussian equation constants from the fit, the amplitude of the worm motion, the standard deviation, and the location of the peak were determined. This process was repeated for the next consecutive peak, and the difference between the two peaks produced the wavelength.

Results and Discussion

Our model was able to determine basic locomotive parameters to describe the model of *C. elegans* during their four most common modes of motion: straight motion, the shallow turn, the omega turn, and the reversal. The wavelength, amplitude, and worm speed were determined for the motion of two different worms using the techniques detailed in the Methods section. One worm (CS) was used as the control, examining its motion as it moved without any external stimuli. The second worm (SS) was used to test the reaction of *C. elegans* to photo-stimulation by examining the motion before and after temporary light fluctuations. Comparing these modes of locomotion for both stimulated and unstimulated worms is a good test for the accuracy of the wave model and can help quantify the neural differences between spontaneous and evasive motion.

During the observation period, the most frequent mode of motion by count and duration was the shallow turn. Spontaneous reversals were the least frequent mode of locomotion, with the CS worm only performing one brief spontaneous reversal. The control and pre-photo reversal data represent locomotion performed in the absence of external stimuli for the CS and SS worms, while the post-photo data represent the post-phototaxis locomotion of the SS worm. Although both worms were roughly age-matched, the CS worm was longer than the SS worm and so there were significant differences in the parameters. Even after normalizing the data to the relative length of the worms, the parameters for the CS worm were considerably smaller than the parameters of motion for the SS worm. This discrepancy between worms could mean that the parameters of locomotion change with biological development. Thus when reading the

histograms, it is important to compare the relative trends in motion across locomotive modes rather than comparing the CS worm to the SS worm.

Figure 10 presents the average worm speed for different modes of locomotion for the CS and SS worms. The error bars represent the average standard deviation determined from the linear regression, and the numbers on the columns reference the number of movements used for each calculation. As the worms deviated from straight motion and performed shallow or omega turns, their speed increased slightly. A significant difference in worm speed was observed when comparing the backward, linear velocities of reversals to the forward linear velocity of straight motion. For example, the average reversal velocity for the SS worm under no stimulation was nearly 62% faster than its average worm speed for straight motion. Worm speed was also shown to noticeably increase when comparing straight motion to omega turns.

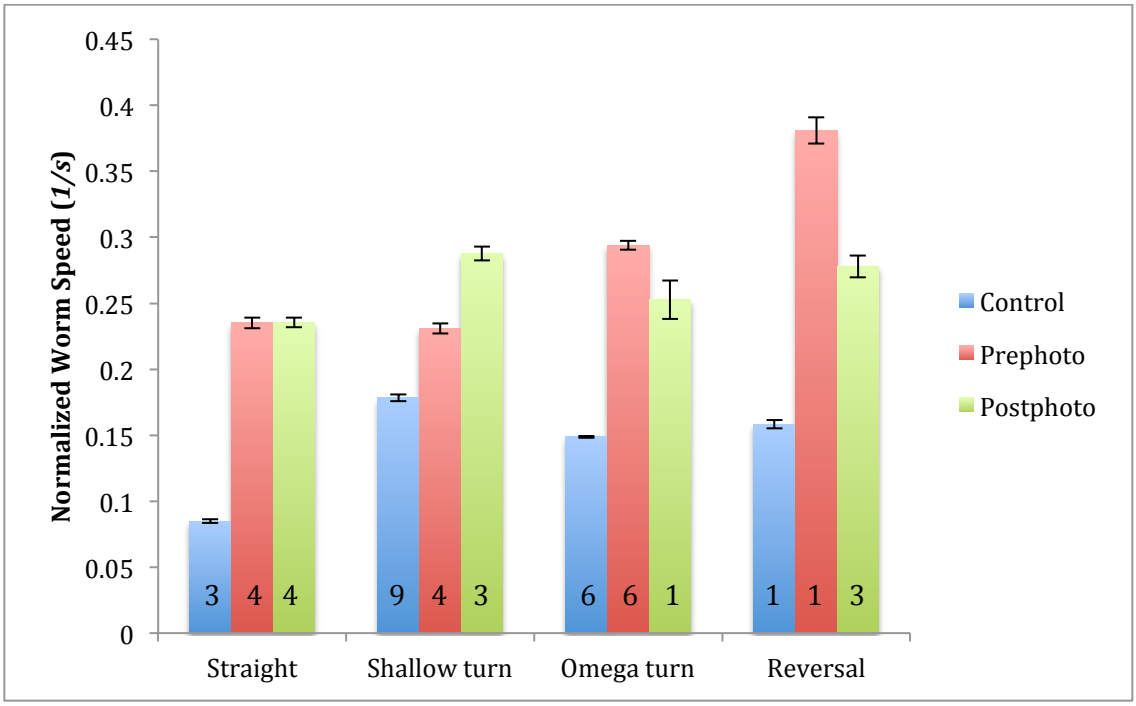

Figure 10. Weighted averages of the worm speed for the CS and SS worms for four modes of locomotion: straight, shallow turns, omega turns, and reversals. The weighted averages of the errors in the linear regressions are represented as error bars. The numbers along the bars represent the number of events per locomotive mode (n).

The significant difference in speed between straight motion and straight reversal motion could be due to a biological difference in the motor muscles that are being used to execute each motion. The increased speed during omega turns could also be a product of a biological survival mechanism used to reduce worm vulnerability. When the worm is contorted in the omega shape, it is physically restricted until the completion of the turn, leaving itself vulnerable. Thus, *C. elegans* temporarily speeds up to finish the turn and move into a safer position.

Additionally, the worm speed was found to significantly decrease during phototaxis. To show this behavior in isolation, similar locomotive parameters found in one of the SS worm videos were compared with and without the stress of photo

stimulation. The most noticeable difference was found when comparing spontaneous reversals to stimulated reversals for one worm, as shown in Figure 11.

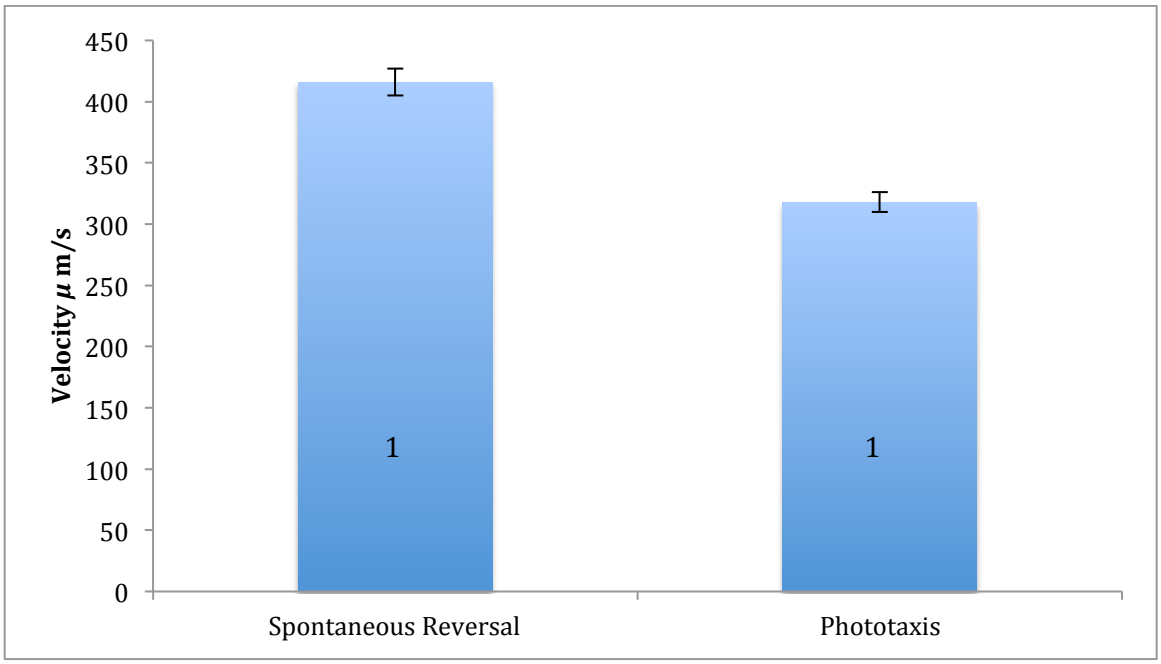

Figure 11. The reversal speed of the SS worm before and after photo stimulation. These two exposures were performed sequentially in the same video.

This points to an inherent behavioral difference between spontaneous and evasive motion and the neural activity that dictates each respective motion. The difference exhibited in Figure 11 is a quantitative expression of two different neural behaviors in the worm: spontaneous motion versus evasive motion. Spontaneous reversal locomotion is activated by VNC motor neurons in coordination with interneurons (28). Meanwhile, evasive reversal locomotion due to photo-stimulation occurs from a combination of ASJ photo sensory neurons in coordination with interneurons and motor neurons (28).

C. elegans have the ability to habituate themselves to their environment, so over time the worm became accustomed to the light-varying environment (29). To observe this time-dependent behavior, consecutive phototaxis responses of the SS worm were

compared for one video. The habituation of the worm is shown in Figure 12, where the phototaxis response quickly decreased over the course of three photo-stimulations.

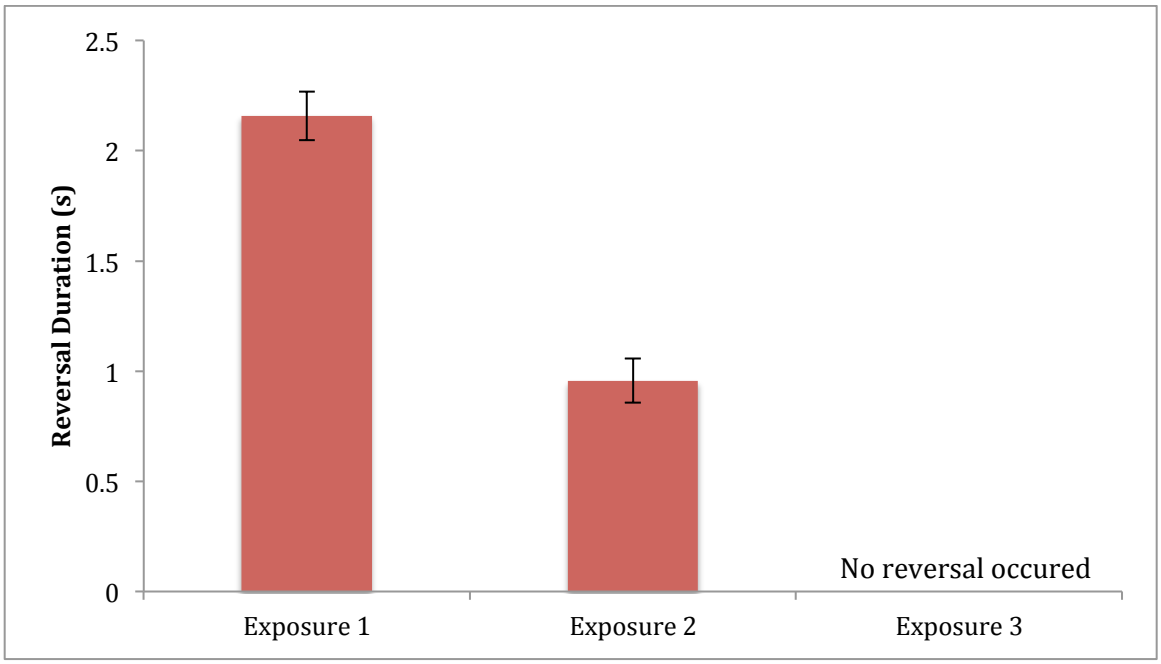

Figure 12. The reversal duration of a stimulated worm during multiple exposures. These three exposures were performed sequentially in the same video. The error bars represent the uncertainty in the duration measurement.

After the first few trials, the worm stopped reacting to the stimulus in any noticeable way.

The locomotive parameters of wavelength and amplitude were also examined across locomotive modes for CS and SS worms. However, these parameters were much less conclusive or informative. In Figure 13 A, the average wavelengths are shown for different locomotive modes. As mentioned previously, spontaneous reversals were the least common locomotive mode, with only one spontaneous reversal occurring for the CS worm. The duration of the reversal was too short to find the wavelength or amplitude of its motion, which is why there is no reversal control data.

When comparing the wavelength of the CS worm across different modes of locomotion, its wavelength remained consistent within the error. Similarly, when comparing the wavelength of the SS worm across different locomotive modes, with and

without stimulation, no significant difference was observed. This wavelength regularity for different locomotive modes is consistent with current literature and point to an optimal wavelength of motion due to the worm's biomechanics and fixed dendrite length of the motor neurons (22).

Figure 13 B presents the amplitude of worm motion during different modes of locomotion before and after photo stimulation. Our determination of the worm amplitude was inconclusive due to large variation in the error bars. Both the wavelength and amplitude parameters were found from the Gaussian fit, so the error from the Gaussian function applied to both. Since worm amplitude is much smaller than wavelength, the error in the amplitude determination is much more significant.

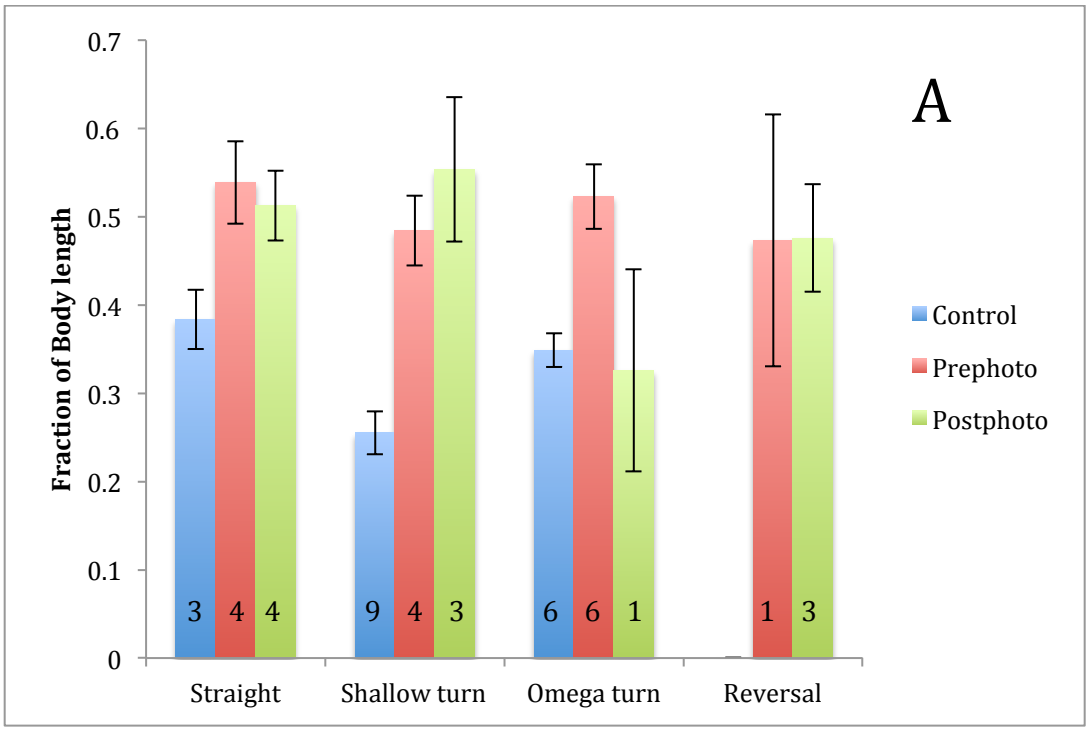

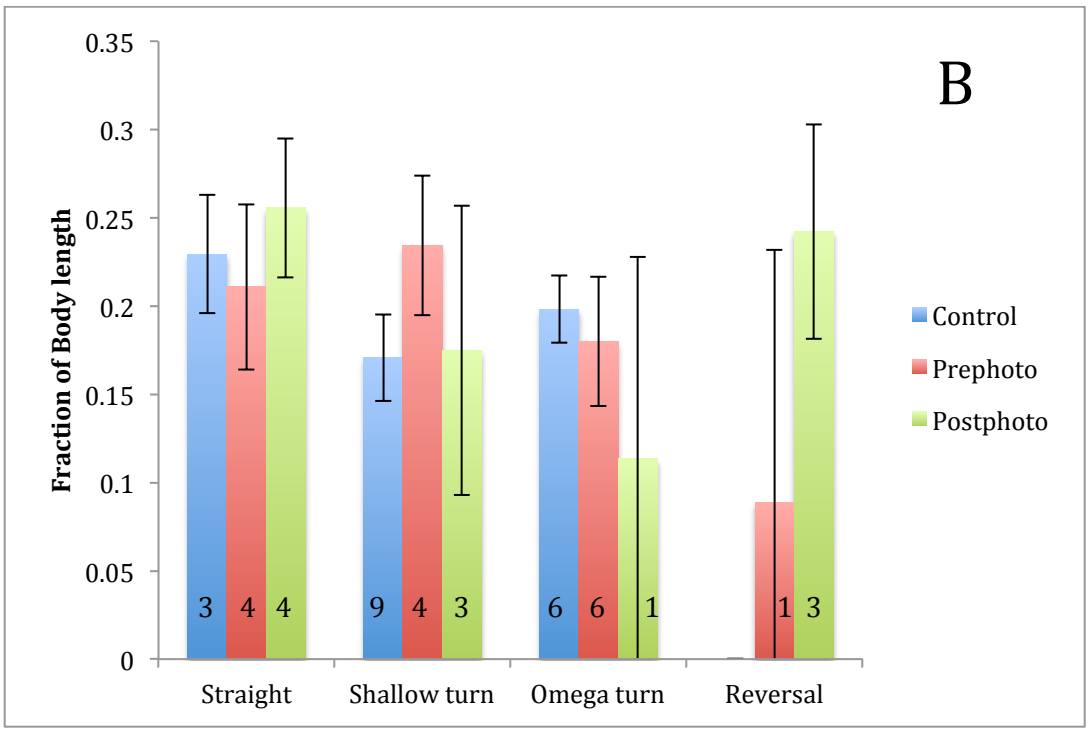

Figure 13. Weighted averages of the A) wavelengths and B) Amplitudes for the CS and SS worms for four modes of locomotion: straight, shallow turns, omega turns, and reversals. There is no CS reversal data because the only reversal performed by the CS worm was too short for an accurate calculation. The weighted averages of the errors in the Gaussian fit are represented as error bars. The numbers along the bars represent the number of events per locomotive mode (n).

The error in Figure 13 represent the standard deviation found when fitting Gaussian functions to sinusoidal curves. Using a Gaussian function for curve fitting is ideal when identifying the parameters of the curve such as peak and amplitude. However the drawback of fitting a sinusoidal curve to a Gaussian function is that the Gaussian bell curve will never look like a sinusoidal wave, regardless of the quality of our data collection. An example of the fit of a perfect Gaussian function and sine functions can be found in the Appendix. Thus, there will always be error in the fit. The more curved the wave motion is, the more significant the error will be, which is why there was significant variation in the error.

Due to this large variation in error, the amplitude data is inconclusive. Especially for parameters where the n number was smaller, one or two wide sinusoidal curves made the error much larger than it should be. Further studies might look into increasing the population size to see if the error bars decrease. The wavelength of the worm remains the same across all locomotive modes; so to increase its velocity during these turns the worm might be modulating its frequency of motion.

Concluding Remarks

One of the primary goals of neurobiology is to understand how animals respond to their environment. The most obvious behavioral output for animals is through locomotion, and so detailed analysis of their fundamental locomotory modes is a helpful tool when investigating animal response to external stimuli. *C. elegans* have recently emerged as ideal model organisms for the study of photo sensory systems due to the fact that they have no eyes but are photosensitive. Light stimulus has been shown to elicit evasive locomotive behavior in C. elegans, however little research has been done to quantify this movement. Recent locomotive analysis of *C. elegans* has ranged from specific, quantitative studies determining the eigenmodes of worm shape, to more descriptive, general analyses of locomotive mode frequency (8,12). This study attempted to integrate both types of analysis, offering a simple model for identifying locomotive phenotypes.

In its current form, our model is incapable of providing the details necessary for a thorough functional locomotive screen. Our results revealed that worm speed is a promising parameter that can be used to differentiate between certain fundamental locomotive modes, and between spontaneous and evasive motion. Significant differences

in worm speed were observed between straight motion, turns, and reversals, however the distinction between shallow and omega turns was minimal. The amplitude and wavelength data was far less conclusive, with large error bars making it difficult to identify any patterns. To strengthen the conclusions of this study, future studies should analyze more data from each worm, as well as analyze more worms. Additionally, alternative methods for curve fitting should be explored to decrease the size of the error in the wavelength and amplitude data. Finally, future studies should explore the accuracy and precision of this current wave model by exploring *C. elegan* locomotive response to other stimuli.

Appendix 1

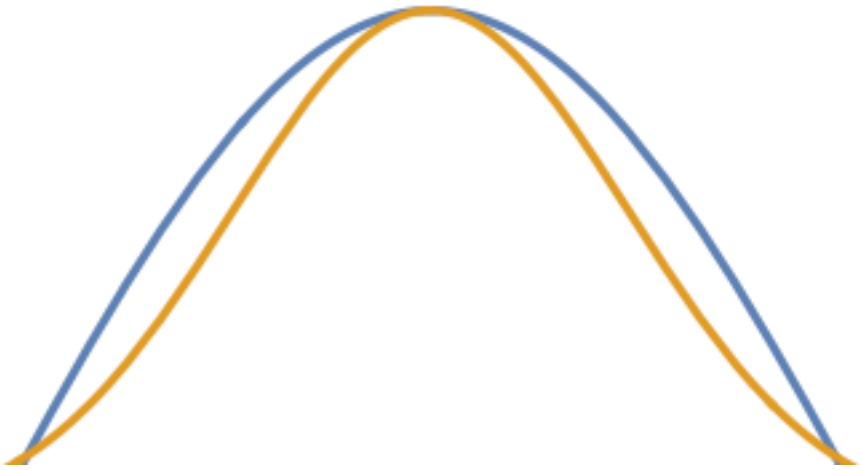

Figure 14: A Gaussian function fitted to a perfect sine curve. The blue line represents the sine curve while the yellow line represents the Gaussian function. This graph represents an inherent limitation in our fit due to the fundamental difference between the two functions.

Appendix 2

Error Analysis:

Curve fitting, also known as regression analysis, is often used to find the "best fit" line or curve for a series of data points. Typically the purpose of the fit is to produce an equation that describes the points anywhere along the curve. Least Squares is one popular method of curve fitting that minimizes the square of the error between the original data and the values predicted by the equation. A major weakness of the Least Squares method is that it is sensitive to any outliers in the data. Thus, if one data point is separate from the majority of the data, then the regression can be skewed. Fortunately, due to the inherent biological constraints of locomotion, all worm data was general uniform.

To extract the amplitude, wavelength, and worm speed from the motion of the *C. elegans* worm, mathematical functions were used to describe every movement of the worm. As mentioned in the methods section, the data from the Tracker software produced two plots: the position of the worm head along the y-axis versus time (Figure 7), and the position of the worm head along the y-axis and x-axis independent of time (Figure 8). The speed of the worm can be represented as a change in distance (Δy) over a change in time (Δt) as shown in Equation 7

$$v = \frac{\Delta y}{\Delta t}. \tag{7}$$

Since the worm is moving at a constant velocity along the y-axis, the data in Figure 7 is linear and the slope of the data is equal to the speed of the worm.

Linear regression:

A linear regression is a statistical method used to model the relationship between a dependent variable and an independent variable. Performing a linear regression consists of finding the equation for best-fitting straight line through a series of points, called a regression line. For this study, Excel data analysis software was used to perform a least squares linear regression. The regression for one set of data is shown in Figure 15.

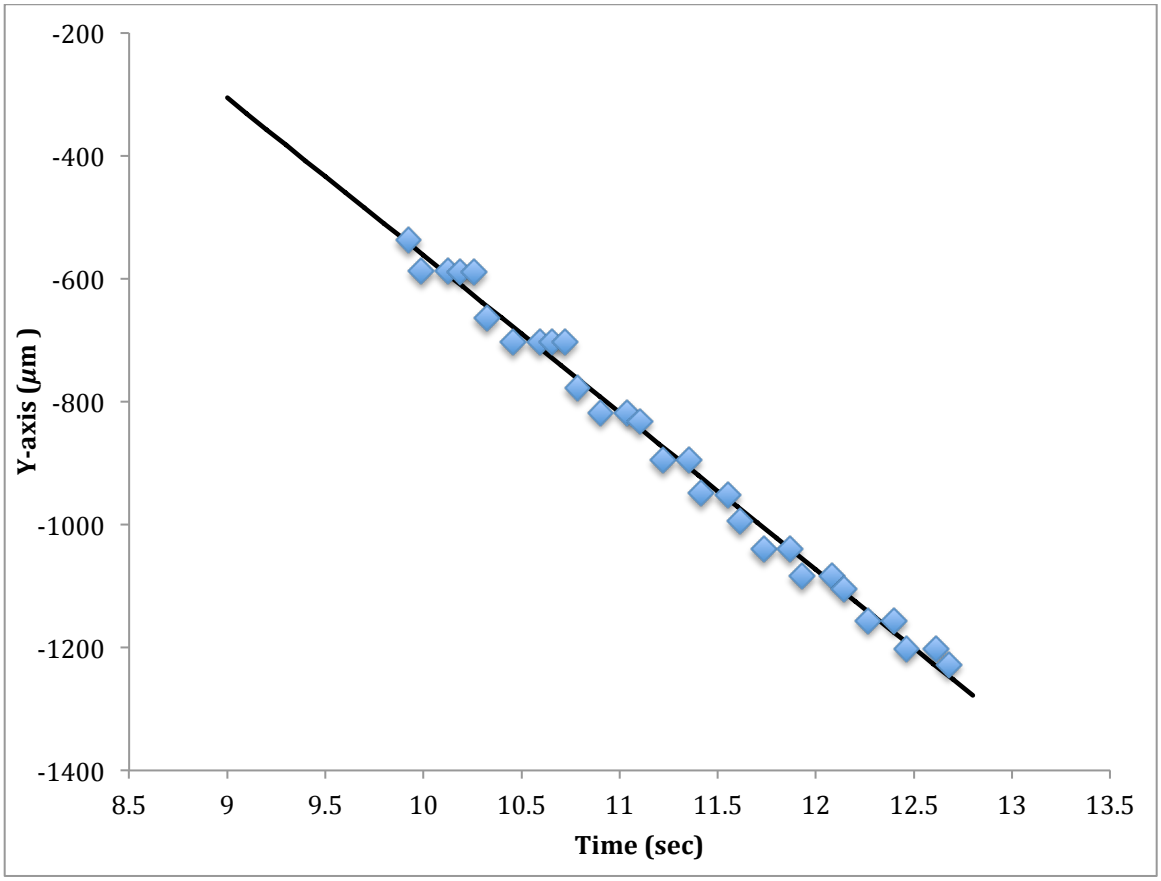

Figure 15: The motion of the worm along the y-axis over time. The linearity of the data shows that the worm is moving at a constant speed. A linear regression was used to find the slope of the line, which represents the speed of the worm.

The output from the Excel program is shown in Table 1 and Table 2. Table 1 contains a list of parameters that detail how well the linear regression fit the data.

Table 1: The parameters from the output of the Excel linear regression. These parameters detail how well the regression line fits with the data.

Regression Statistics	
Multiple R	0.995139412
R Square	0.990302449
Adjusted R Square	0.989943281
Standard Error	21.91391713
Observations	29

The multiple R is the correlation coefficient, which represents how strong the linear relationship is. R squared is the coefficient of determination, which represents how many points fall on the regression line. The adjusted R-square adjusts for the number of terms in a model. The standard error of the regression is an estimate of the standard deviation of the error. The standard error of the regression is the precision that the regression coefficient is measured. Observations are the number of data points used in the regression.

In Table 2, the coefficients for the equation of the regression are shown in the first column. The standard errors of the coefficients are shown in the second column. In this case, the intercept refers to the y-intercept of the regression line, while the X-variable refers to the slope of the regression line.

Table 2: The coefficients for the equation of the regression line. These were also part of the output for Excel linear regression.

	Coefficients	*Standard Error*	*t Stat*	*P-value*
Intercept	1996.123141	54.97515311	36.30955128	1.86347E-24
X Variable 1	-255.7824051	4.871199195	-52.50912452	1.00959E-28

Based on the information in Table 2, the slope of the line, which is the speed of the worm, is 255.78 μm. The negative sign is relative to the orientation of the coordinate system and can be disregarded, as we are only concerned about the magnitude of the

worm speed. The error in the slope is 4.87 μm, meaning that the slope of the regression line is an accurate fit with the data.

To find the wavelength and amplitude of the worm motion, the peaks of the curves needed to be determined. While a least squares linear regression is a standard way to fit a line to a set of linear data, there multiple ways to fit non-linear equations to curved data.

Estimation By Hand

One simple method for determining the peak of a curve is to take the average of the two points that appear closest to the peak. The uncertainty in the peak is based on the uncertainty in the measurements, which is 4 μm in the Tracker software. The uncertainty in the measurements can be propagated using the following equation

(8) $$dE = \sqrt{{\sigma_1}^2 + {\sigma_2}^2}$$

where σ_2 is the error for one measurement, σ_1 is the error for the other measurement, and dE is the uncertainty in the peak.

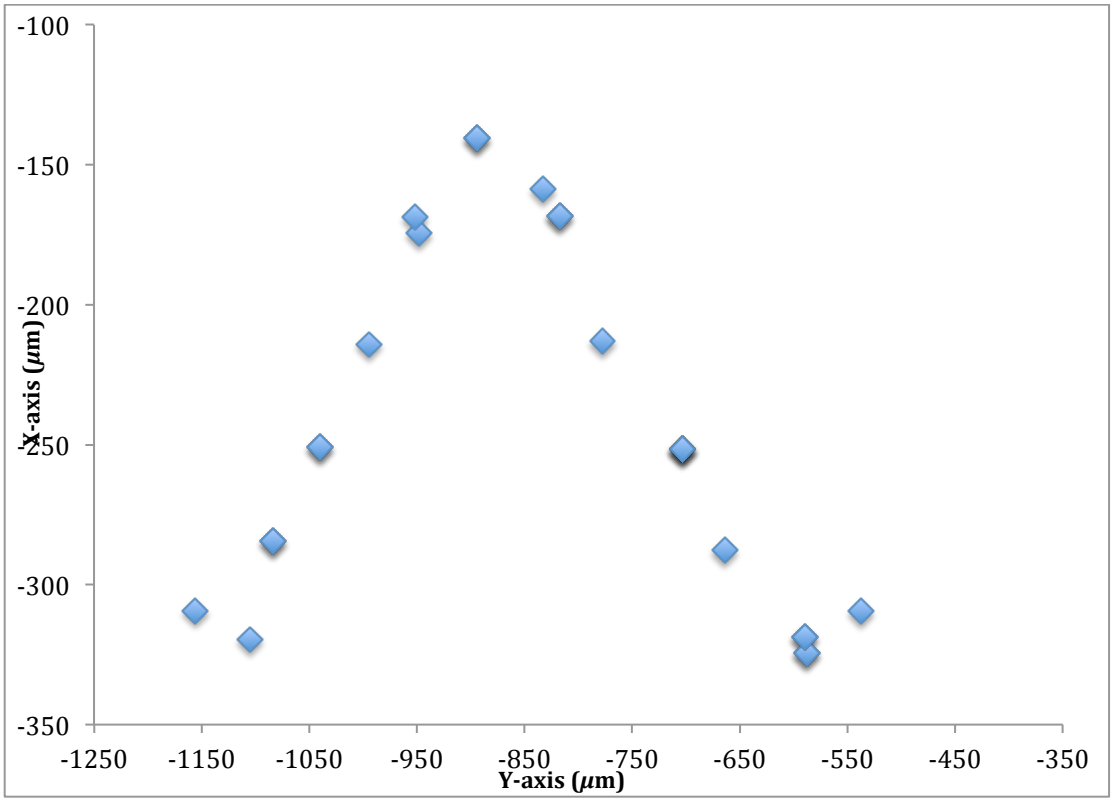

Figure 16: A graph of the worm path traced by the head. Each data point represents the position of the head for one time frame.

For the curve shown in Figure 16, the calculated wavelength and amplitude was $652 \pm 4\ \mu m$ and $180 \pm 4\ \mu m$. However these values are rough estimations and are not up to the caliber of quantitative analysis desired for this study.

Gaussian Fit

Instead, we chose to fit a Gaussian equation to the curve, minimizing the root mean square error corresponding to the parameters of the fitted Gaussian equation. The equation for a Gaussian function can be found in the methods section (Equation 6). Root means square is a method used to describe how closely the fitted function resembles the data. The root mean square error can be determined by the equation:

(9) $$Error = \sqrt{\frac{1}{n}\sum_{i=1}^{n}(y_i - f(x_i))^2},$$

where n is the number of data points, y_i is the experimental data point and $f(x_i)$ is the theoretical data point corresponding to the experimental x_i value. Using Excel's solver software, the parameters of a given equation can be optimized to match the experimental data series. The result of fitting a Gaussian curve to the experimental data in Figure 16 is shown in Figure 17.

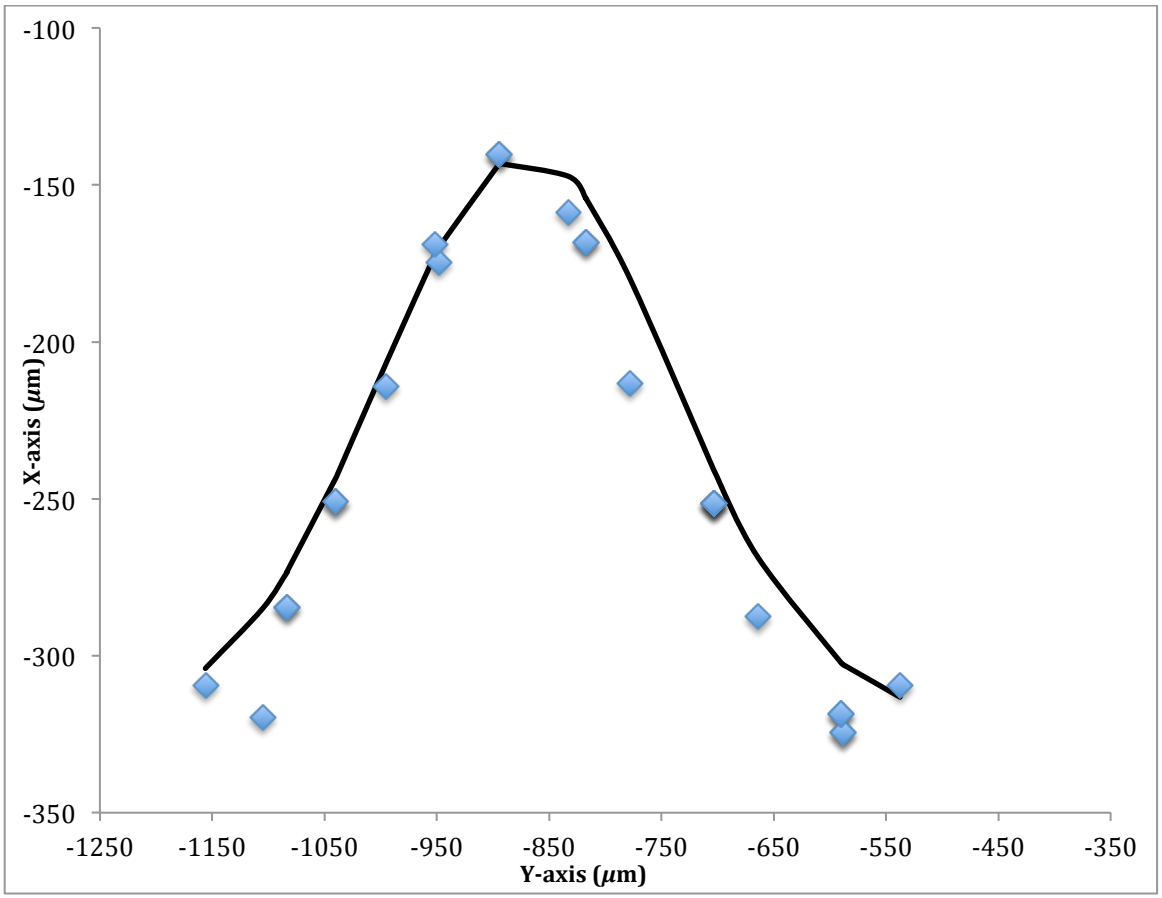

Figure 17: A graph of the worm position and the corresponding Gaussian fit. The experimental data is represented by the blue points, while the black line represents the theoretical Gaussian curve. From this line, a Gaussian equation was used to find the peak of the curve. From this peak, the wavelength and the amplitude of motion were determined.

The optimized equation for the Gaussian fit is

(10) $$y = -320 + 180e^{\frac{-(x+870)^2}{2(130)^2}}.$$

Based on this expression, the standard deviation is 130 μm, the amplitude is 180 μm and the position of the peak along the y-axis is -870 μm. To find the wavelength, the same fit was done to an adjacent curve and the difference between the two y values was determined. The resulting wavelength was 665 μm. The error in the wavelength was propagated using Equation 8 and found to be 180 μm.

For the error in the amplitude, initially the standard deviation from the Gaussian fit was used. All of the figures in the results sections were made using those values. However, sigma overestimated the error in the amplitude, as seen in Figure 13. Since the sigma represents the standard deviation in the y-direction, the standard deviation along the x-axis was determined by taking the difference between the peak and the height of the Gaussian function at the maximum and minimum standard deviations. Subtracting the y-axis deviation of 130 μm from the location of the peak, -740 μm and -1000 μm were the maximum and minimum deviations. Substituting these new values back into the Gaussian expression, the height of the function on each side was found to be -211 μm at the maximum and minimum deviation, equating to 71 μm less than the maximum amplitude. Compared to the standard deviation associated with the wavelength (130 μm), 71 μm is an improvement.

When deciding what fit to use, we considered two other fits. The first fit was a fast Fourier transform. The second fit was a sine wave.

Fast Fourier Transform

The idea behind a Fourier fit is that any function can be expressed as a series of sine and cosine curves. The Fourier transform of the plot of the x-position versus time is shown below. A Fourier transform detects the frequency at which the Fourier function best

resonates at, identifying the exact frequency of the peak. It is important to note that Fourier fits cannot determine amplitudes.

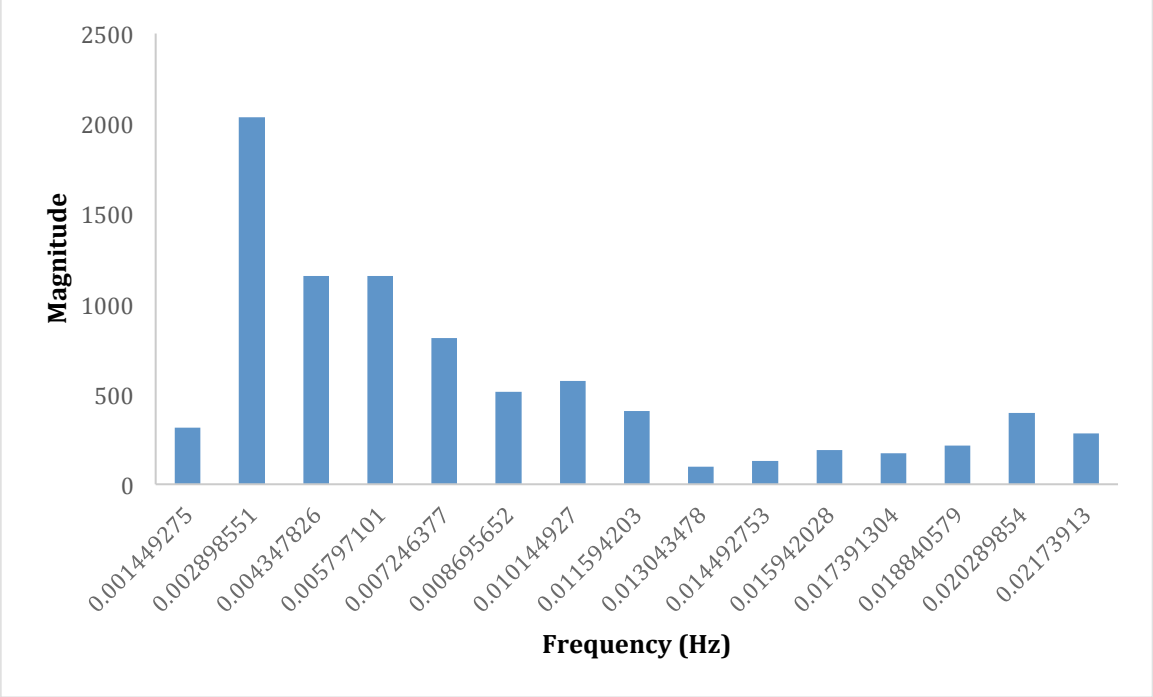

Figure 18: A Fourier transform of the position of the worm head along the x-axis over time. The most significant harmonic frequency was 0.00289 Hz.

From this plot, the most significant harmonic frequency was found to be 0.00289 Hz. Frequency is related to wavelength using the following equation:

(11) $$\lambda = \frac{v}{f}.$$

Using the worm speed found from the linear regression earlier in the appendix, the wavelength using the Fourier fit was found to be 677 μm. This is close to the value found with our Gaussian. To test the validity of the fit, root mean squared error was used. The error in this wavelength was found to be 0.4 μm, which is much smaller than the error found using the Gaussian fit. While this is the most accurate method of curve fitting, it is also the most complicated. One of the goals of this study was to provide a model of analysis that is accessible to the scientific community, and many biologists

would not be able to quickly and easily perform Fourier transforms. We chose to utilize the Gaussian fit for the purpose of this study since it provided similar determinations for the wavelength and amplitude.

Sinusoidal Fit

Since the wave model of this study assumes that the worm moves in a sinusoidal form, we also attempted to fit the motion of the worm to a sine function as shown in Figure 19.

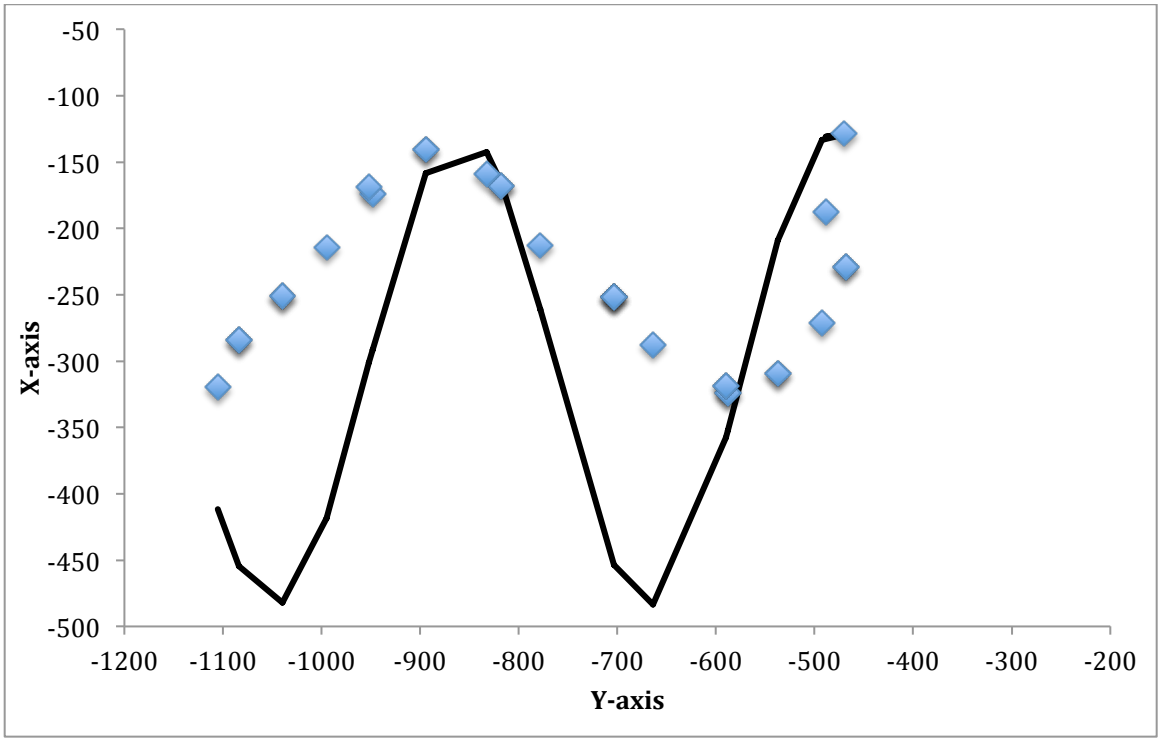

Figure 19: A graph of the worm position and the corresponding sine wave fit. The experimental data is represented by the blue points, while the black line represents the theoretical sine wave. The equation for the sine wave was used to find the peak of the curve. From this peak, the wavelength and the amplitude of motion were determined.

At first, one would expect that the sinusoidal fit is the most accurate, since the wave model assumes sinusoidal motion. However due to the fact that *C. elegans* are living and imperfect, the worm motion is generally sinuous rather than sinusoidal. Thus, fitting sine waves over multiple curves won't produce an accurate fit. Even when fitting the sine wave to one or two data curves at a time, the root mean square error was optimized so

that the entire sine function matched with the data. This is why the fitted sine wave is not matched at the peak as shown in Figure 19. Performing this analysis on another curve, the wavelength was calculated at $650 \pm 99\ \mu m$ and the amplitude was found to be $178 \pm 99\ \mu m$. A summary of the analysis results can be found in Table 3.

Table 3: A summary of the curve fitting methods tested in this study. The Gaussian fit was the one used for the results shown in the body of the paper.

	Fourier Fit	Gaussian Fit	Sinusoidal Fit	By Hand
Pro	Provides the most accurate fit.	Fits peak very precisely.	Resembles worm path	Easiest to perform, mathematically simple.
Con	Least accessible to general scientific community	Overestimates error with sigma value.	Worm path is sinuous. Bad fit for curve peak.	Least accurate/statistically sound.
Measured Wavelength	$677 \pm 0.4\ \mu m$	$665 \pm 180\ \mu m$	$650 \pm 99\ \mu m$	$652 \pm 4\ \mu m$

Works Cited

1. Alberts, B. http://www.ncbi.nlm.nih.gov/books/NBK26818/

2. Significance of Animal Behavior Research.
http://www.csun.edu/~vcpsy00h/valueofa.htm

3. Ward, A., Liu, J., Feng, Z., & Xu, X. Z. Light-sensitive neurons and channels mediate phototaxis in C. elegans. http://www.ncbi.nlm.nih.gov/pmc/articles/PMC2652401/

4. Search Deep Blue. Retrieved April 29, 2016, from
https://deepblue.lib.umich.edu/handle/2027.42/77700

5. Ward, A., Liu, J., Feng, Z., & Shawn Xu, X. Z. (2008). Light-sensitive neurons and channels mediate phototaxis in *C. elegans*. *Nature Neuroscience*, *11*(8), 916–922.
http://doi.org/10.1038/nn.2215

6. "Using Model Organisms to Study Health and Disease." - National Institute of General Medical Sciences. Web. 23 Mar. 2016.
https://www.nigms.nih.gov/Education/Pages/modelorg_factsheet.aspx

7. Lobo, I. (2008) Biological complexity and integrative levels of organization. Nature Education 1(1):141

8. Dujon, B. 1996. The Yeast Genome Project: What Did We Learn? Trends in Genetics. 12.7: 263-70.

9. Lai, Chun-Hung et al. 2005. Identification of Novel Human Genes Evolutionarily Conserved in *Caenorhabditis Elegans* by Comparative Proteomics. Genome Research 10.5: 703–713.

10. Hobert, Oliver. "Specification of the Nervous System*." Worm Book. Web. 03 Apr. 2016. http://www.wormbook.org/chapters/www_specnervsys/specnervsys.html.

11. Kuwabara, P. E., and N. O'Neil. 2001. The Use of Functional Genomics in C. Elegans for Studying Human Development and Disease. J. Inherited Metabolic Disease. 24.2: 127-38.

12. "Locomotion of C. Elegans Worm to Make Big Difference in Biomedical Research." News-Medical.net. American Institute of Physics, 16 Oct. 2013. Web. 23 Mar. 2016.

13. Stephens G.J., B. Johnson-Kerner, W. Bialek, W.S. Ryu. 2008. Dimensionality and Dynamics in the Behavior of *C. elegans*. *PLoS Computational Biology*. 4.4

14. Kaletta, T. and M.O. Hengartner. 2006. Finding Function in Novel Targets: C. Elegans as a Model Organism. Nat Rev Drug Discov 5.5: 387-99.

15. The C.elegans Sequencing Consortium. 1998. Genome Sequence of the Nematode C. Elegans: A Platform for Investigating Biology. Science. 282.5396: 2012-018.

16. Durbin, R. and E.L.L., Sonnhammer. 1997. Analysis of Protein Domain Families in *Caenorhabditis elegans*. Genomics. 46.2: 200-212.

17. Kim, D., S. Park, L. Mahadevan, and J. H. Shin. 2011. The Shallow Turn of a Worm. J. Exp. Bio. 214: 1554-1559.

18. Fang-Yen, C., et. al. 2010. Biomechanical analysis of gait adaptation in the nematode *Caenorhabditis elegans*. PNAS. 107.47: 20323-20328.

19. Schulman, R.D., M. Backholm., W.S. Ryu., and K. Dalnoki-Veress. 2014. Dynamic force patterns of an undulatory microswimmer. Phys. Rev. E. 89.5: 050701.

20. Sznitman, J., X. Shen., P.K. Purohit., P.E. Arratia. The Effects of Fluid Viscosity on the Kinematics and Material Properties of *C. elegans* Swimming at Low Reynolds Number. Society for Experimental Mechanics. 50:1303–1311.

21. Zhen, M., and A.D. Samuel. 2015. C. Elegens Locomotion: Small Circuits, Complex Functions. Current Opinion in Neurobiology. 33: 117-126.

22. Peliti, M., J.S. Chuang, S. Shaham. 2013. Directional Locomotion of C. elegans in the Absence of External Stimuli. PLOS One. 8(11).

23. Padmanabhan, V. et. al. 2012. Locomotion of C. Elegans: A Piecewise-Harmonic Curvature Representation of Nematode Behavior. PLoS ONE. 7.7

24. Pak, On Shun, and Eric Lauga. "CHAPTER 4. Theoretical Models of Low-Reynolds-Number Locomotion." RSC Soft Matter Series Fluid-Structure Interactions in Low-Reynolds-Number Flows: 100-67. University of Cambridge. Web. 3 Apr. 2016.

25. Korta, J., D. A. Clark, C. V. Gabel, L. Mahadevan, and A. D. T. Samuel. 2007. Mechanosensation and Mechanical Load Modulate the Locomotory Gait of Swimming C. Elegans. Journal of Experimental Biology 210.13: 2383-389.

26. Sznitman, J., Purohit, P. K., Krajacic, P., Lamitina, T., & Arratia, P. E. (2010). Material Properties of *Caenorhabditis elegans* Swimming at Low Reynolds Number. *Biophysical Journal*, *98*(4), 617–626.

27. Karbowski, J., Cronin, C. J., Seah, A., Mendel, J. E., Cleary, D., & Sternberg, P. W. (2006). Conservation rules, their breakdown, and optimality in Caenorhabditis sinusoidal locomotion. Journal of Theoretical Biology, 242(3), 652-669.

doi:10.1016/j.jtbi.2006.04.012

28. Park, Juyong, Deok-Sun Lee, and Marta C. González. "The Eigenmode Analysis of Human Motion." J. Stat. Mech. Journal of Statistical Mechanics: Theory and Experiment 2010.11 (2010). Web.

29. Gulla, J. 2011. Modeling the Wave Motion of a Guitar String. http://www.forskningsradet.no/servlet/Satellite?blobcol=urldata&blobheader=application%2Fpdf&blobheadername1=ContentDisposition%3A&blobheadervalue1=+attachment%3B+filename%3D%22GullaJanFys.pdf%22&blobkey=id&blobtable=MungoBlobs&blobwhere=1274491693086&ssbi

30. Alternating Current (AC) vs. Direct Current (DC). (n.d.). Retrieved April 10, 2016, from https://learn.sparkfun.com/tutorials/alternating-current-ac-vs-direct-current-dc/alternating-current-ac

31. The Equation of a Traveling Wave. 2016. http://www.physics.byu.edu/faculty/christensen/Physics 220/FTI/16 Wave Motion/16.6 The equation of a traveling wave.htm

32. Brenner, S. 1974. The Genetics of *CAENORHABDITIS ELEGANS*. Genetics. 77(1):71-94.

33. Handbook - Nervous System General Description.2016 http://www.wormatlas.org/hermaphrodite/nervous/mainframe.htm#NeuroFIG6

34. Zhao, B., Khare, P., Feldman, L., & Dent, J. A. (2003). Reversal frequency in Caenorhabditis elegans represents an integrated response to the state of the animal and its environment. Journal of Neuroscience, 23(12), 5319-5328.

35. Beale E, Li G, Tan MW, Rumbaugh KP (2006) Caenorhabditis elegans senses bacterial autoinducers. Applied and environmental microbiology 72: 5135–5137.

36. Riddle, Donald L. (1997) *C. Elegans II*. Plainview, NY: Cold Spring Harbor Laboratory.

37. Pennisi, E. (1998). Worming secrets from the *C. elegans* genome. Science, 282, 1972-1974.

38. Cronin, Christopher J., Jane E. Mendel, Saleem Mukhtar, Young-Mee Kim, Robert C. Stirbl, Jehoshua Bruck, and Paul W. Sternberg. (2015). "An Automated System for Measuring Parameters of Nematode Sinusoidal Movement." *BMC Genetics*. BioMed Central, 7 Feb. 2005.

39. Eisenmann, D. M. (2005). Locomotion WormBook, 1.7.1, http://www.wormbook.org.